Correlation of Fractionation Tray Performance via a Cross-Flow Boundary-Layer Model

Thomas C. Young and Warren E. Stewart
Dept. of Chemical Engineering, University of Wisconsin, Madison, WI 53706

The nonequilibrium tray model proposed by Young and Stewart (1990) is used to correlate published fractionation data from sieve tray columns 0.45 m to 1.2 m in diameter. The model contains a dimensionless coefficient a_{00} to describe the interphase heat and mass transfer, and a Peclet number Pe to describe the lateral mixing of the liquid on the tray. The coefficient a_{00} is investigated as a function of tray geometry and hydrodynamic variables, using an error-in-variables extension of a multiresponse parameter estimation algorithm. Data from several sources are well correlated by a simple dimensionless relation for a_{00}, with Pe predicted from the results of Bennett and associates (1983, 1991).

Introduction

In a recent article (Young and Stewart, 1990), we gave a new model and computation scheme for predicting temperatures and compositions on cross-flow fractionation trays. Here we use these tools to analyze published fractionation data and develop predictive correlations for computer-aided process design.

Tray efficiencies are used commonly in reporting tray performance and in various methods for column calculations. The merits and limitations of various efficiency forms for these purposes are well documented (Standart, 1965; Holland and McMahon, 1970; King, 1980; Krishnamurthy and Taylor, 1985), as are the difficulties of generalizing tray efficiencies to multicomponent systems (Toor and Burchard, 1960; Holland, 1963; Holland and McMahon, 1970; Miskin et al., 1972).

Mechanistic models of tray performance, such as the present one, use transfer coefficients rather than tray efficiencies. This approach facilitates the application of current knowledge from transport theory and eliminates calculations of extraneous equilibrium states. Similar conclusions were reached by Krishnamurthy and Taylor (1985) in their development of a nonequilibrium tray model. Tray efficiencies remain convenient for comparisons of observations with model predictions, and we will give such comparisons later on.

Several models have been given by previous investigators to relate whole-tray performance to point conditions. The well-mixed tray model, the mixing-pool model (Nord, 1946), the recirculation model (Oliver and Watson, 1956), and the eddy diffusivity model (AIChE, 1958) have all been used to approximate the liquid mixing patterns on a tray. For ease of solution, each of these models was restricted to linear equilibrium, uniform temperature, and transfer coefficients on a tray, zero net molar interphase transfer and two-component mixtures. Young and Stewart (1990) developed a cross-flow boundary-layer model and a collocation scheme to simulate large trays efficiently without these restrictions. The liquid-phase dispersion coefficient used in their model may be predicted for sieve trays from the correlations of Bennett and associates (1983, 1991).

Interphase transfer models used in previous work include the penetration model (Higbie, 1935), the surface-renewal model (Danckwerts, 1951), eddy diffusivity models (Földes and Evangelidi, 1968; Hughmark, 1971), and annular two-phase flow models (Bakowski, 1952; Krishna, 1985; Young and Weber, 1972). Each of these models requires a separate correlation of the transfer coefficients for each phase, since the ratios of the vapor and liquid coefficients are not predicted *a priori*. In the present work, we avoid this difficulty by using the boundary layer theory of Stewart et al. (1970), which predicts the transfer coefficients for each phase as corresponding functions of the interfacial geometry and motion. A single measurable function a_{00} (Stewart, 1987) summarizes the main effects of interfacial geometry and motion on the mass and energy exchange between the phases. Young and Stewart (1990) extended this model to multicomponent, nonisothermal sys-

Correspondence concerning this article should be addressed to W. E. Stewart.
Current address of T. C. Young: The Dow Chemical Company, 2800 Mitchell Drive, Walnut Creek, CA 94598.

tems with varying bulk states on each tray; here we use a simplified version of the model to analyze binary fractionation on nearly isothermal trays.

In correlation work, calculated tray efficiencies have often been treated as original data. This approach can give difficulty, because the variances of tray efficiencies depend strongly on the operating conditions and are largest for runs with small composition changes across the test section. It is better to fit the postulated model directly to the measured stream states to facilitate proper weighting and allow better mass-balance adjustments. Here we fit each model to the original data and include a variance for each observation; this is known as an "error-in-variables" approach.

In the following sections, the tray model and chosen data are reviewed. Then, the coefficient a_{00} defined in this model is investigated as a function of the hydrodynamical variables of a fractionating tray. Fractionation data from three laboratories are well fitted by the model with simple dimensionless expressions for a_{00}.

Basic Tray Model

The cross-flow model given by Young and Stewart (1990) is used. One-dimensional liquid flow across the tray is assumed, with dispersion caused by splashing. The vapor is assumed to flow vertically through the liquid without backmixing. Vapor mixing above each tray is assumed to be complete, but the computation method can easily handle more complex assumptions. Froth and clear liquid heights are treated as uniform across the tray, as is the molar density of each phase. Comments and corrections to our earlier article (Young and Stewart, 1990) are given in Appendix II.

The model is applied here in simplified binary form. Conductive energy transport is neglected, and the bulk and interfacial fluids are assumed to be at their saturation temperatures. Comparisons of this version with the full model indicate that the fitted values of a_{00} agree within a few percent as long as the fluids entering the tray are close to saturation. All data used here meet this condition.

The resulting steady-state continuity equations for the bulk vapor and bulk liquid are as follows:

$$v_G^* \frac{\partial y_{A,\infty}}{\partial z^*} = \frac{A_0}{\mathfrak{W}_{G,\mathrm{ref}}} (k_{A,G}^{\bullet} + N_{T0,G})(y_{A,0} - y_{A,\infty}) \tag{1}$$

$$\frac{\partial v_G^*}{\partial z^*} = \frac{A_0}{\mathfrak{W}_{G,\mathrm{ref}}} N_{T0,G} \tag{2}$$

$$\frac{1}{Pe}\frac{\partial^2 x_{A,\infty}}{\partial l^{*2}} - v_L^* \frac{\partial x_{A,\infty}}{\partial l^*} = \frac{\mathfrak{W}_{G,\mathrm{ref}}}{\mathfrak{W}_{L,\mathrm{ref}}} [v_G^*(y_{A,\infty} - x_{A,\infty})|_{z^*=1} - v_G^*(y_{A,\infty} - x_{A,\infty})|_{z^*=0}] \tag{3}$$

$$\frac{\partial v_L^*}{\partial l^*} = -\frac{\mathfrak{W}_{G,\mathrm{ref}}}{\mathfrak{W}_{L,\mathrm{ref}}} (v_G^*|_{z^*=1} - v_G^*|_{z^*=0}) \tag{4}$$

and are subject to the following boundary conditions:

$$y_{A,\infty} = y_{A,\mathrm{in}} \qquad \text{at } z^* = 0 \tag{5}$$

$$v_G^* = 1 \qquad \text{at } z^* = 0 \tag{6}$$

$$x_{A,\infty}|_{0+} - x_{A,\infty}|_{0-} = \frac{1}{Pe}\frac{\partial x_{A,\infty}}{\partial l^*}\bigg|_{0+} \qquad \text{at } l^* = 0 \tag{7}$$

$$\frac{\partial x_{A,\infty}}{\partial l^*} = 0 \qquad \text{at } l^* = 1 \tag{8}$$

$$v_L^* = 1 \qquad \text{at } l^* = 0 \tag{9}$$

The subscript ∞ denotes bulk fluid states, corresponding to the outer limit of the local diffusional boundary layer. The mass-transfer coefficient $k_{A,G}^*$ and net interfacial molar flux $N_{T0,G}$ are based on the reference area A_0 of the tray; thus, $N_{T0,G}A_0$ is the net molar vaporization rate that would result if $N_{T0,G}$ were constant at the given value on all the interfacial area of the tray.

The interphase transfer model is based on the mobile-interface boundary layer theory of Stewart et al. (1970); it gives the following equations for the vapor phase:

$$N_{A0,G} = y_{A0}N_{T0,G} + k_{A,G}^{\bullet}(y_{A0} - y_{A\infty}) \tag{10}$$

$$k_{A,G}^{\bullet} = k_{A,G}\frac{\exp(-\phi_{A,G}^2/\pi)}{[1 + \mathrm{erf}(\phi_{A,G}/\sqrt{\pi})]} \tag{11}$$

$$k_{A,G} = c_G \mathfrak{D}_{AB,G}^{1/2} a_{00}\sqrt{V/L} \tag{12}$$

$$N_{T0,G} = \phi_{A,G}k_{A,G} \tag{13}$$

$$a_{00} = \frac{2}{\sqrt{\pi}}\frac{1}{A_0}\sqrt{L/V}\iint_{\mathfrak{R}}\frac{\partial}{\partial t}\sqrt{\int_{t_0(u,w)}^{t} s^2(u,w,t_1)dt_1}\,du\,dw \tag{14}$$

Corresponding equations hold for the liquid phase, with the same function a_{00} and with the subscript G replaced by L. The reference quantities L, V and A_0 are chosen here as the outlet weir height h_w, the inlet superficial vapor velocity $\langle v_G \rangle$, and the tray projected area A_{tray}, respectively.

Equation 13 relates the interphase transfer function a_{00} to the interfacial motion, with time-dependent area $s(u, w, t)$ $dudw$ for each surface element $dudw$ in the interfacial region $\mathfrak{R}(u, w, t)$ of a single tray. The surface function $s(u, w, t)$ is not available except for simple flows, so the function a_{00} must be found by other means. We treat a_{00} here as a pseudo-steady function to be correlated by fitting the theory to experiments.

Equations 12 and 13, and their liquid-phase analogs give the relation

$$\phi_{A,L} = -\frac{\mathfrak{D}_G}{c_L}\left(\frac{\mathfrak{D}_{AB,G}}{\mathfrak{S}_{AB,L}}\right)^{1/2}\phi_{A,G} \tag{15}$$

when the mass balance in Eq. 16 is used. The normal fluxes relative to the interface satisfy the conservation conditions:

$$\begin{bmatrix} N_{A,0} \\ e_0 \end{bmatrix}_G = -\begin{bmatrix} N_{A,0} \\ e_0 \end{bmatrix}_L \tag{16}$$

Table 1. Tray Specifications

	Garrett	Ahmed	FRI 8%	FRI 14%
Tray diameter (cm)	45.7	59.0	120.0	120.0
Hole diameter (cm)	0.635	0.476	1.270	1.270
Hole pitch (cm)	1.78	1.27	3.81	3.02
Exit weir height (cm)	2.54	5.00	5.08	5.08
	5.08		2.54	2.54
	7.62			
Inlet weir height (cm)	0	2.50	0	0
Open area (cm^2)	147.7	185.0	715.7	1,178.0
Active tray area (cm^2)	1,152	2,001	8,590	8,590
Tray area (cm^2)	1,254	2,001	8,590	8,590
Liquid path length (cm)	30.9*	37.4	76.2	76.2
Tray height (cm)	45.7	60.0	61.0	61.0
Exit weir width (cm)	22.9	45.7	94.0	94.0
Downcomer area (cm^2)	99.4	344.0	1,400	1,400

* Estimated

Here the conductive contribution to e_0 is neglected, giving $e_0 = N_{A,0}\,\overline{H}_{A,0} + N_{B,0}\overline{H}_{B,0}$ on each side of the interface. This interfacial energy balance calls for net molar transfer unless the molar latent heats of species A and B are equal. Finally, the equilibrium condition

$$y_{A,0} = K_A x_{A,0} \tag{17}$$

completes the interfacial boundary conditions for this simplified model.

Young and Stewart (1990) gave a collocation procedure for solving their basic tray model and achieved good accuracy with just two collocation points per tray. The same procedure is used here for the simplified model in Eqs. 1-17.

Description of Data

The data used in this work were obtained from four performance studies of large-diameter circular sieve trays done by Sakata and Yanagi (1979), Yanagi and Sakata (1982), Garrett (1975), and Ahmed (1982). The tray specifications are listed in Table 1. Sieve tray data were selected because of the nonproprietary nature of these tray designs and their widespread use in industry. Small-diameter tray data were not used, because the wall effects in such experiments are not representative of industrial trays.

Sakata and Yanagi (1979) and Yanagi and Sakata (1982) reported detailed data on the performance of 120-cm-dia. sieve trays for distillation of two hydrocarbon systems at various pressures. This work was done at the Fractionation Research Institute in a column providing up to ten trays. Test trays with 8% and 14% open area were used. All tests were conducted at total reflux. Cyclohexane and *n*-heptane were used at 27.6, 34.5 and 165 kPa; *n*-butane and isobutane were used at 1,138, 2,068 and 2,760 kPa. The butane system also contained as much as 14.7 mol % propane in some tests.

Table 2. FRI Data Used in This Work

No. of Runs	p (kPa)	h_w (cm)	Open Area (%)	No. of Trays	Plot Symbol
		Cyclohexane-n-Heptane			
7	165.0	5.08	8	7	○
4	27.6	5.08	8	7	×
3	165.0	5.08	8	4	△
3	34.5	5.08	8	4	□
3	34.0	2.54	14	3	◇
		n-Butane-Isobutane			
5	1,138.0	5.08	8	7	▽
		n-Butane-Isobutane-Propane			
4	1,138.0	5.08	14	6	+

Liquid compositions in the downcomers were measured in the FRI efficiency tests, along with reboiler and reflux liquid compositions. No vapor compositions were reported. The first (top) tray was used as an entrainment collection tray, and the reflux was introduced on the second tray, usually in a subcooled condition. The vapor feed to the bottom tray was reported to be close to saturation. All trays, but the top two, are considered representative of normal operation. The column was designed with large downcomers, so flooding was expected to be governed by entrainment.

The FRI data (Sakata and Yanagi 1979; Yanagi and Sakata 1982) cover a wide range of operating conditions. The results used here were selected from the total-reflux efficiency tests and some of the entrainment tests. Runs with flooding, high entrainment, or weeping were omitted. Runs with small to moderate entrainment rates were handled by the methods described by Young (1990).

Few downcomer composition measurements were reported for the cyclohexane-heptane total reflux runs at 165 kPa on the 14% open-area tray, so those runs were not used. Many of the reported downcomer compositions for the cyclohexane-heptane total-reflux efficiency tests at 34 kPa on the 14% open-area tray indicated negative tray efficiencies, so those measurements were not used. The *n*-butane-isobutane-propane runs at 2,068 and 2,760 kPa were omitted because the supercritical component (propane) could not be handled by the thermodynamic property estimation methods used here. Hoek and Zuiderweg (1982) have also suggested that vapor entrainment in the downcomers may be a problem in those runs. Twenty-five binary column tests and four ternary tests, summarized in Table 2, were selected as representative of normal operation.

Garrett (1975) reported detailed data on the distillation of two nonideal binary systems near atmospheric pressure on a 45.7-cm-dia. sieve tray. Some of these data are discussed by Anderson et al. (1976) and by Garrett et al. (1977). The two binary systems (toluene-*n*-propanol and *n*-propanol-benzene) were intended to be representative of the two classes of surface-tension-active systems defined by Zuiderweg and Harmens (1958); however, calculations by the methods described in Appendix A indicate only minor variations of surface tension in these systems. Factorial experimental designs were used to study the effects of weir height, internal reflux ratio and vapor flow rate for each binary. Total reflux tests were also performed for each binary from 15% to 97.5% of flooding with a 2-in. (51-mm) weir.

Garrett calculated vapor flow rates from an energy balance and the steam condensation rate in the reboiler. Tests with other than total reflux were performed by recycling liquid from the reboiler to the condensor or vice versa. Vapor compositions were sampled at three points above and three points below the test tray, and liquid compositions were sampled in each downcomer. The compositions of liquid recycle streams were also

measured. The three compositions for a vapor stream often disagree significantly, and mass balance closures on the test tray are sometimes poor. Composition errors seem most severe at low vapor flow rates (15-30% of flooding), perhaps because of weeping.

Garrett calculated tray efficiencies from the averaged vapor compositions. The measured liquid compositions were tabulated, but were not used. Since no reason was given for this, the liquid and vapor compositions are treated here as having equal variances, and the reported tray efficiencies are not used.

The downcomers in Garrett's column appeared to be relatively small, and the flow rates were relatively low; these considerations suggest that flooding was governed by downcomer backup. Consequently, we have neglected entrainment in our treatment of these data. The test tray had significant dead area behind the downcomers and had no inlet weir. There was also a high proportion of inactive area around the edges of the tray, which may have caused liquid bypassing or recirculation on the tray.

Garrett provides data from 55 sieve tray tests. Two were set aside because they were taken at 15% of flooding, where weeping may be substantial. Two other tests (no. 109 and no. 219) were eliminated because of severe mass balance problems. The remaining 51 tests were used.

Ahmed (1982) reported detailed data on the performance of a 60-cm-dia. sieve tray for the distillation of methanol and water at atmospheric pressures. These data are discussed by Lockett and Ahmed (1983). Particular attention was given to composition measurements. Vapor compositions were sampled above and below the test tray. Liquid compositions were sampled in the downcomer, at the exit weir, and at several other points on the test tray.

Liquid compositions at the exit weir were found to differ substantially from those in the downcomer. Lockett and Ahmed attributed this difference to vaporization in the downcomer, caused by heat transfer from the tray below. They developed three models based on mass and energy balances around the tray and downcomer, and used the results of their models to correct the observed compositions. The details of these calculations are given by Ahmed (1982), along with tables of overall heat-transfer coefficients required in their models to produce the observed composition differences. The reported heat transfer coefficients are very high, ranging from 0.12 to 2.5 W/cm^2·K. These high values were attributed to nucleate boiling in the downcomer; however, the reported temperature differences of less than 15 K between trays are too small to support nucleation. It seems more likely that these composition differences were caused by sampling difficulties at the exit weir.

The measured downcomer liquid compositions are used here without Ahmed's correction. In this form, all 35 runs reported by Ahmed appear to be reasonably accurate and representative of normal sieve tray operation.

Parameter Estimation

The distillation data described above contain measured compositions and flow rates of liquid, vapor and recycle streams. Since each of these measurements is subject to error, the conditions of the runs are uncertain. Therefore, in this study we have estimated the run conditions as part of the parameter set for each model investigated.

Table 3. Implementation of Error-in-Variables Method

Observed Response	Predicted Response
y_{in}	$\tilde{y}_{in} = \theta_1$
y_{out}	$y_{out} = \tilde{y}_{out}(\theta_1, \theta_2, \theta_3, a_{00}, Pe)$
x_{in}	$\tilde{x}_{in} = \tilde{x}_{in}(\theta_1, \theta_2, \theta_3, a_{00}, Pe)$
x_{out}	$\tilde{x}_{out} = \tilde{x}_{out}(\theta_1, \theta_2, \theta_3)$
x_R	$\tilde{x}_R = \theta_2$
$\mathcal{W}_R/\mathcal{W}_G$	$\tilde{\mathcal{W}}_R/\tilde{\mathcal{W}}_G = \theta_3$

The method used to model the observations is shown schematically in Table 3. Each binary run includes observations of two to six of the listed responses, which are modeled with the corresponding predictor functions. Sakata and Yanagi (1979) and Yanagi and Sakata (1982) gave multitray data, all at total reflux with observations of the third and fourth responses. Garrett (1975) gave single-tray data, some at total reflux with observations of the first four responses, and some with liquid recycle around the tray with observations of all six responses. Ahmed (1982) gave single-tray data, all at total reflux with observations of the first four responses.

For each distillation run a parameter θ_1 was introduced, as shown in Table 3, to model the composition of entering vapor. For each run with other than total reflux, two additional parameters were introduced: θ_2 to model the composition of the recycle stream and θ_3 to model the ratio of the recycle and inlet vapor flow rates. The predicted responses $\tilde{y}_{out}$ and $\tilde{x}_{in}$ were calculated from the tray model (in multitray form when needed), using these run parameters along with the parameters in the candidate expressions for a_{00}. The predicted response $\tilde{x}_{out}$, which was computed from a material balance around the test section, depends only on the parameters θ_1, θ_2 and θ_3 of the given run. Thus, the full parameter vector θ for each model reported in this work consisted of the hydrodynamic parameters for a_{00} plus the relevant parameters θ_i of Table 3 for each included run.

The observations from each laboratory form a separate data block Y_b, in which the errors are treated as independent, unbiased, and Normally distributed. For want of replicate data, equal variances are assumed here for all observations from a given laboratory.

The combined data form a block-rectangular array of 432 rows and three columns:

$$Y = \begin{bmatrix} Y_1 & 0 & 0 \\ 0 & Y_2 & 0 \\ 0 & 0 & Y_3 \end{bmatrix} \tag{18}$$

Table 4. Ranges of Dimensionless Groups

	FRI	Garrett	Ahmed
$\rho_G\langle v_G\rangle h_w/\mu_L$	76–5,500	50–890	92–220
$(A_{act}/A_{open})^2 - 1$	52 and 143	60	116
ρ_G/ρ_L	0.0014–0.058	0.0030–0.0056	0.00069–0.0011
μ_G/μ_L	0.013–0.095	0.017–0.025	0.019–0.031
$\langle v_G\rangle^2/(gh_w)$	0.025–21	0.21–7.6	3.9–18
$\sigma/(\rho_L g h_w d_h)$	0.006–0.0087	0.0033–0.012	0.012–0.018
w_L/w_G	1	0.44–1.7	1

Table 5. Modeling of a_{00} for the FRI Data

NPa	Model	Deg. of Freedom	Residual Sum of Squares
1	$a_{00}=243.7$	24	0.1149
2	$a_{00}=0.0133\left(\frac{\rho_G\langle v_G\rangle h_w}{\mu_G}\right)^{0.959}$	23	0.0131
2	$a_{00}=5.52\left(\frac{\rho_G\langle v_G\rangle h_w}{\mu_L}\right)^{0.541}$	23	0.00741
3	$a_{00}=0.585\left(\frac{\rho_G\langle v_G\rangle h_w}{\mu_L}\right)^{0.734}\left(\frac{\rho_L}{\rho_G}\right)^{0.199}$	22	0.00397
3	$a_{00}=0.396\left(\frac{\rho_G\langle v_G\rangle h_w}{\mu_L}\right)^{0.733}\left(\frac{\mu_L}{\mu_G}\right)^{0.399}$	22	0.00350
3	$a_{00}=6.43\left(\frac{\rho_G\langle v_G\rangle h_w}{\mu_L}\right)^{0.612}\left(\frac{\mu_L\langle v_G\rangle}{\sigma}\right)^{0.159}$	22	0.00287
3	$a_{00}=3.40\left(\frac{\rho_G\langle v_G\rangle h_w}{\mu_L}\right)^{0.619}\left(\frac{\langle v_G\rangle^2}{gh_w}\right)^{0.082}$	22	0.00287
25	Individual a_{00} values	0	0.00000

The block Y_1 consists of 25 sets of observed values x_{in} and x_{out} selected from Sakata and Yanagi (1979) and Yanagi and Sakata (1982). The block Y_2 consists of 32 sets of observed values y_{in}, y_{out}, x_{in}, x_{out} and 19 sets of observed values y_{in}, y_{out}, x_{in}, x_{out}, x_R and $\mathcal{W}_R/\mathcal{W}_G$ taken from Garrett (1975). The block Y_3 consists of 35 sets of observed values y_{in}, y_{out}, x_{in}, x_{out} taken from Ahmed (1982).

If the relative variances of the three data collections were known, they could be combined into a single vector and fitted by weighted least squares with the various candidate models. Since the relative variances were not known, it proved more direct to use a multiresponse criterion provided by Box and Draper (1965, 1972). This criterion takes the form of a posterior probability density function $p(\theta \mid Y)$ for the parameter vector θ of the postulated model, conditional on the given data matrix Y. For the present form of Y, the function given by Box and Draper (1972) reduces to:

$$p(\theta \mid Y)=(\text{const})\prod_{b=1}^{3}[SS_b(\theta)]^{-n_b/2} \tag{19}$$

in which SS_b is the sum of squared residuals, $[Y_{ub}-f_{ub}(\theta)]^2$, over the n_b observations in data block b for the given model function f. For a single data block, this approach leads to a least-squares computation, and the statistical procedures described by Draper and Smith (1981) can be applied; therefore, the following discussion deals only with the combined treatment of all three blocks via Eq. 19.

The most probable estimate, $\hat{\theta}$, of the parameter vector for a given model and given data Y is that which maximizes the posterior density $p(\theta \mid Y)$. This estimate also minimizes the related objective function of Stewart et al. (1988),

$$S'(\theta)=-2\ln p(\theta \mid Y)+\text{const}'=\sum_{b=1}^{3} n_b \ln[SS_b(\theta)\nu_{b,\text{ref}}/\nu_b] \tag{20}$$

Table 6. Modeling of a_{00} for the Data of Garrett

NPa	Model	Deg. of Freedom	Residual Sum of Squares
1	$a_{00}=64.9$	155	0.1355
2	$a_{00}=0.344\left(\frac{\rho_G\langle v_G\rangle h_w}{\mu_G}\right)^{0.571}$	154	0.0922
2	$a_{00}=3.78\left(\frac{\rho_G\langle v_G\rangle h_w}{\mu_L}\right)^{0.546}$	154	0.0902
3	$a_{00}=0.143\left(\frac{\rho_G\langle v_G\rangle h_w}{\mu_L}\right)^{0.516}\left(\frac{\rho_L g d_h^2}{\sigma}\right)^{1.11}$	153	0.0899
3	$a_{00}=3.41\left(\frac{\rho_G\langle v_G\rangle h_w}{\mu_L}\right)^{0.570}\left(\frac{gh_w}{\langle v_g\rangle^2}\right)^{0.051}$	153	0.0895
3	$a_{00}=3.62\left(\frac{\rho_G\langle v_G\rangle h_w}{\mu_L}\right)^{0.555}\left(\frac{w_L}{w_G}\right)^{0.189}$	153	0.0894
3	$a_{00}=3.41\left(\frac{\rho_G\langle v_G\rangle h_w}{\mu_L}\right)^{0.592}\left(\frac{\sigma}{\mu_L\langle v_G\rangle}\right)^{0.134}$	153	0.0893
52	Individual a_{00} values	104	0.0817

Table 7. Modeling of a_{00} for the Data of Ahmed

NPa	Model	Deg. of Freedom	Residual Sum of Squares
1	$a_{00}=122.6$	114	0.0314
2	$a_{00}=6.72\left(\frac{\rho_G\langle v_G\rangle h_w}{\mu_L}\right)^{0.591}$	113	0.0194
2	$a_{00}=0.329\left(\frac{\rho_G\langle v_G\rangle h_w}{\mu_G}\right)^{0.670}$	113	0.0159
3	$a_{00}=0.114\left(\frac{\rho_G\langle v_G\rangle h_w}{\mu_L}\right)^{0.610}\left(\frac{\rho_L g d_h^2}{\sigma}\right)^{1.96}$	112	0.0132
3	$a_{00}=0.00630\left(\frac{\rho_G\langle v_G\rangle h_w}{\mu_L}\right)^{0.640}\left(\frac{\mu_L}{\mu_G}\right)^{1.72}$	112	0.0129
3	$a_{00}=3{,}210.0\left(\frac{\rho_G\langle v_G\rangle h_w}{\mu_L}\right)^{-0.155}\left(\frac{\mu_L\langle v_G\rangle}{\sigma}\right)^{0.817}$	112	0.0125
35	Individual a_{00} values	70	0.00906

which includes a heuristic penalty for addition of parameters. Here ν_b is the number of degrees of freedom for the residuals in block b. In this work, we have assigned ν_1 as $50-(NPa+25)$, ν_2 as $242-(NPa+89)$, and ν_3 as $140-(NPa+35)$, where NPa is the number of parameters used to represent a_{00}. The reference values $\nu_{b,\mathrm{ref}}$ were calculated with $NPa=0$.

By integration of $p(\theta\mid Y)$ one can calculate parameter intervals that have given probability content, and can find the probability that any particular parameter is positive according to the given data. We have done this by approximating $S'(\theta)$ around its minimum as a quadratic in $(\theta-\hat{\theta})$, and $p(\theta\mid Y)$ correspondingly as (const) exp $[-S'(\theta)/2]$. This approximation yields a Normal posterior distribution of θ, for which the integrals can be evaluated from standard tables (Box and Tiao, 1973). They were calculated with the aid of the parameter estimation package GREG, which is described by Caracotsios (1986) and by Stewart et al. (1991).

Correlation Procedure

Young (1990) gave a dimensional analysis of the conservation equations and boundary conditions for a fractionating tray, and obtained the following dimensionless expressions for a_{00} and Pe,

$$a_{00}=a_{00}\left(Re_G,\ Re_L,\ Fr,\ We,\ \frac{\rho_G}{\rho_L},\ \frac{w_L}{w_G},\ \text{Shape Parameters}\right) \tag{21}$$

$$Pe=Pe\left(Re_G,\ Re_L,\ Fr,\ We,\ \frac{\rho_G}{\rho_L},\ \frac{w_L}{w_G},\ \text{Shape Parameters}\right) \tag{22}$$

for nonreacting fluids with negligible surface viscosity. To

Table 8. Modeling of a_{00} for All the Data

NPa	Model	$S(\hat{\theta})$
1	$a_{00}=118.2$	−859.2
2	$a_{00}=17.2\left(\frac{\rho_G\langle v_G\rangle h_w}{\mu_L}\right)^{0.380}$	−989.9
3	$a_{00}=0.122\left(\frac{\rho_G\langle v_G\rangle h_w}{\mu_L}\right)^{0.640}\left(\frac{A_{\mathrm{act}}^2}{A_{\mathrm{open}}^2}-1\right)^{1.03}$	−1,241.0
4	$a_{00}=0.277\left(\frac{\rho_G\langle v_G\rangle h_w}{\mu_L}\right)^{0.648}\left(\frac{A_{\mathrm{act}}^2}{A_{\mathrm{open}}^2}-1\right)^{0.344}\left(\frac{\rho_L\mu_G}{\rho_G\mu_L}\right)^{0.412}$	−1,283.0
5	$a_{00}=0.733\left(\frac{\rho_G\langle v_G\rangle h_w}{\mu_L}\right)^{0.638}\left(\frac{A_{\mathrm{act}}^2}{A_{\mathrm{open}}^2}-1\right)^{0.250}\left(\frac{\rho_L}{\rho_G}\right)^{0.451}\left(\frac{\mu_G}{\mu_L}\right)^{0.600}$	−1,282.0
5	$a_{00}=0.287\left(\frac{\rho_G\langle v_G\rangle h_w}{\mu_L}\right)^{0.624}\left(\frac{A_{\mathrm{act}}^2}{A_{\mathrm{open}}^2}-1\right)^{0.384}\left(\frac{\rho_L\mu_G}{\rho_G\mu_L}\right)^{0.362}\left(\frac{\langle v_G\rangle^2}{gh_w}\right)^{0.019}$	−1,278.0
6	$a_{00}=0.752\left(\frac{\rho_G\langle v_G\rangle h_w}{\mu_L}\right)^{0.642}\left(\frac{A_{\mathrm{act}}^2}{A_{\mathrm{open}}^2}-1\right)^{0.241}\left(\frac{\rho_L}{\rho_G}\right)^{0.458}\left(\frac{\mu_G}{\mu_L}\right)^{0.615}\left(\frac{w_L}{w_G}\right)^{0.270}$	−1,281.0
6	Best two-parameter a_{00} correlations for individual data sources	−1,383.0
9	Best three-parameter a_{00} correlations for individual data sources	−1,449.0

decouple the fluid mechanics from the transport of energy and species, the physical properties were treated as constants, viscous dissipation was neglected, and the effects of net interfacial mass flux on a_{00} and Pe were neglected. Young also gave a more detailed analysis, including surface-tension gradient effects (Marangoni effects) and the net mass flux effects just named; for simplicity, these effects are not considered here. The ranges of variables covered in each data source are shown in Table 4, in terms of a related set of dimensionless groups.

The functions in Eqs. 20 and 21 were investigated in several stages, with physical properties calculated as described in Appendix I. Each test was first fitted with an individual a_{00} value, using the correlations of Bennett and associates (1983, 1991) to predict Pe. These individual a_{00} values were investigated graphically, and candidate models for a_{00} were formulated. These models for a_{00} were then combined with the basic tray and column models, and were fitted by minimizing $S'(\theta)$. Each combined model was first fitted separately to the data from each source and then simultaneously to all the data. Finally, candidate models for a_{00} and Pe were fitted simultaneously to all the data (Young, 1990). The combined correlations of a_{00} and Pe are not reported here, as the data used proved insufficient for reliable estimation of the Pe function.

Correlation of Data from Single Sources

The fitted a_{00} values for the individual FRI runs are shown in Figure 1; they vary strongly with the dimensionless group $\rho_G \langle v_G \rangle h_w/\mu_L$. The values in each subset of the data are connected by lines and are plotted with the symbols defined in Table 2. Four runs with the ternary system *n*-butane–isobutane–propane are included. The subsets of the data conform reasonably to straight, parallel lines, proportional to a common power function of $\rho_G \langle v_G \rangle h_w/\mu_L$. The different intercepts show the need to include additional variables.

Several power-function forms of Eq. 21 were fitted to the FRI data, as shown in Table 5. At the two-parameter level, the mixed Reynolds number $\rho_G \langle v_G \rangle h_w/\mu_L$ gives a better fit than the vapor-phase Reynolds number $\rho_G \langle v_G \rangle h_w/\mu_G$ does. The three-parameter fits are very good; the last two give RMS deviations of $\sqrt{0.00287/(25 \times 2)} = 0.0076$ mol fraction from the original composition data. The last correlation is demonstrated in Figure 2, which shows the predicted and observed average Hausen stage efficiencies for each run. The four ternary runs from Table 2 are also included in Figure 2, but not in the parameter estimates of Table 5.

The Hausen efficiency is defined (Hausen, 1953; King, 1980) as $(y_{A,\text{out}} - y_{A,\text{in}})/(y_{A,E} - y_{A,\text{in}})$, in which $y_{A,E}$ is the ideal outlet vapor composition obtained by a flash equilibrium calculation with the input streams of the given stage. This efficiency is more suitable for model testing than the Murphree efficiencies are, because it is less sensitive to experimental errors.

Figure 3 shows the fitted a_{00} values for the individual runs of Garrett. Again, there is a strong dependence on the mixed Reynolds number $\rho_G \langle v_G \rangle h_w/\mu_L$. The residual sums of squares and parameter estimates for several models based on Eq. 21 are listed in Table 6. An F-test (Draper and Smith, 1981) gives only 78% probability that the third parameter is positive in the best-fitting three-parameter model.

The best three-parameter correlation of Garrett's data is demonstrated in Figure 4, which shows the predicted and observed Hausen stage efficiencies for each run. Here the observed Hausen efficiency was determined for each run by a least-squares fit of the data with a separate value of a_{00} and the relevant parameters θ_i of Table 3.

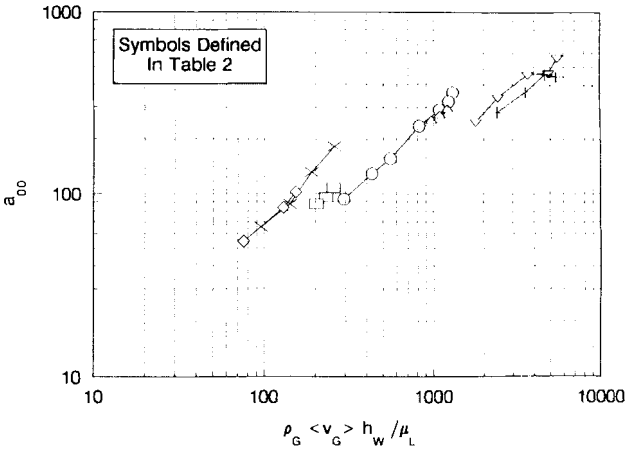

Figure 1. Values of a_{00} fitted to the FRI data.

The transfer parameters calculated from individual runs of Ahmed (1982) are plotted in Figure 5 as values of $a_{00}(\rho_G \langle v_G \rangle h_w/\mu_L)^{-0.5}$ vs. liquid composition. The increase in a_{00} with increasing methanol concentration is suggestive of Marangoni effects, since methanol-water is a surface-tension-positive system as defined by Zuiderweg and Harmens (1958). The operation is reported to be in the froth regime (Lockett and Ahmed, 1983), so it meets the criterion of Fane and Sawistowski (1968) for Marangoni enhancement of separation to be possible in a surface-tension-positive system. An increase of point efficiencies with methanol concentration in methanol-water fractionation was also observed by Kalbassi et al. (1987).

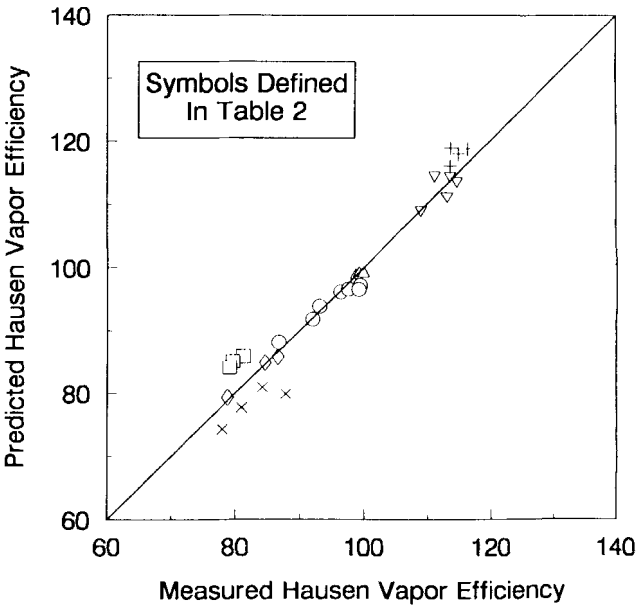

Figure 2. Predicted vs. observed average tray efficiency for the FRI data.

Using the best three-parameter a_{00} expression and the D_E correlation of Bennett and Grimm.

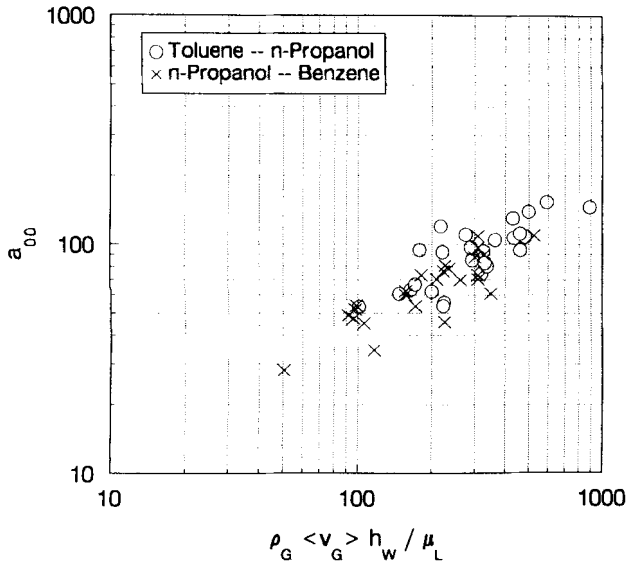

Figure 3. Values of a_{00} fitted to the data of Garrett.

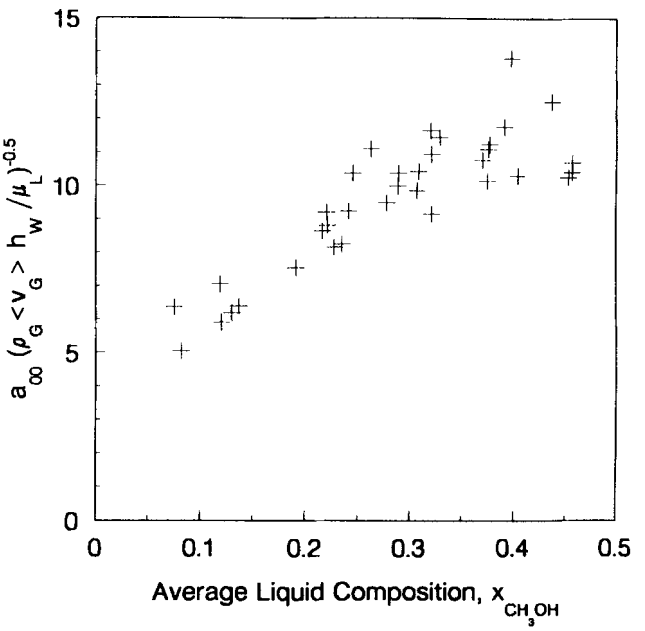

Figure 5. Composition dependence of a_{00} for the data of Ahmed.

The trend in Figure 5 might have simpler causes, however, expressible in the variables of Eq. 21. The present study focuses on those variables, in search of the simplest correlations that will adequately describe the data.

Table 7 shows the results of fitting the data of Ahmed (1982) with various models for a_{00}. Application of the F-test to the last two columns indicates that three parameters are significant at well above the 99.95% probability level. The accuracy of the best three-parameter correlation of these data is demonstrated in Figure 6.

Correlation of the Combined Data

The data of Ahmed, Garrett and FRI were combined into the form of Eq. 18 and treated by the multiresponse methods described for that data structure. As before, the liquid-phase Peclet number Pe was predicted from the correlations of Bennett and associates (1983, 1991). The parameters for each model were estimated by minimizing the objective function $S'(\theta)$ of Eq. 20.

The various fitted models for a_{00} are summarized in Table 8. The best objective-function value is obtained with the four-parameter model, which is reproduced here along with the 95% probability interval for each parameter.

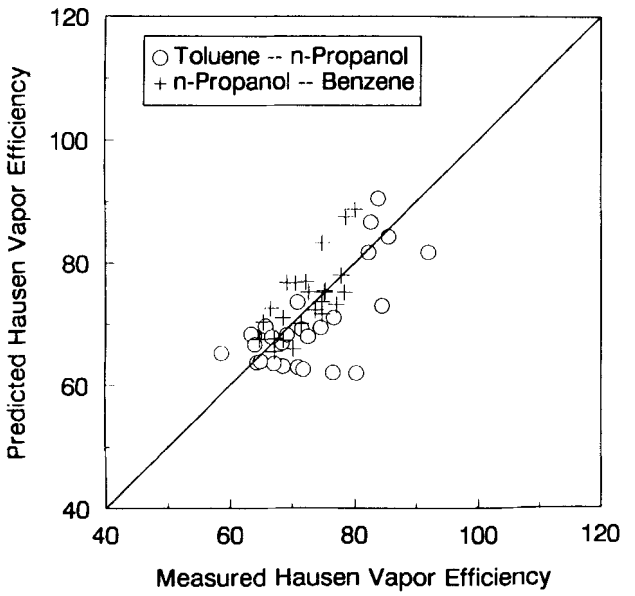

Figure 4. Predicted vs. observed tray efficiency for the data of Garrett.

Using the best three-parameter a_{00} expression and the D_E correlation of Bennett and Grimm.

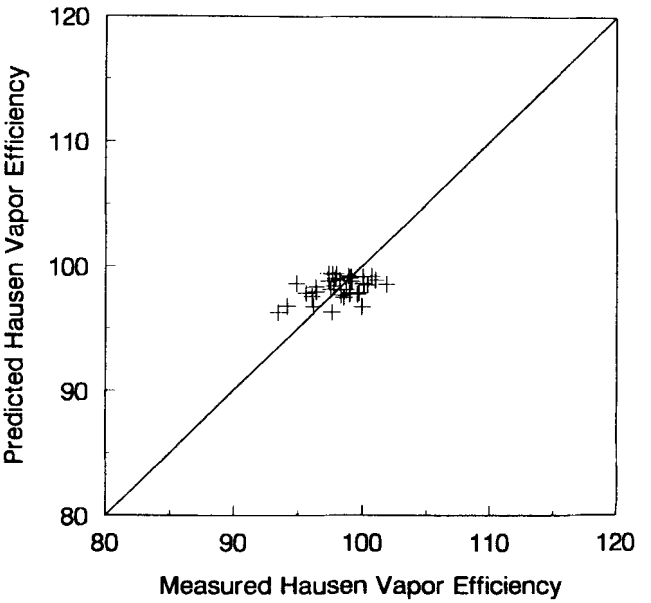

Figure 6. Predicted vs. observed tray efficiency for the data of Ahmed.

Using the best three-parameter a_{00} expression and the D_E correlation of Bennett and Grimm.

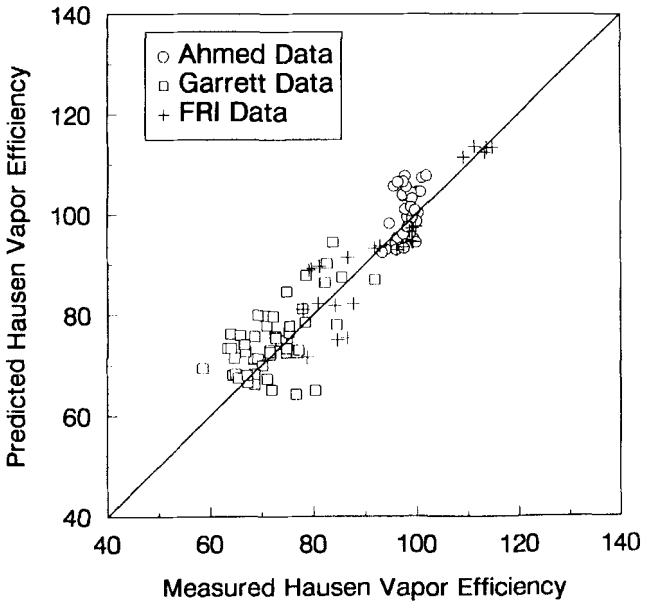

Figure 7. Predicted vs. observed tray efficiency for all the data.

Using Eq. 23 and the D_E correlation of Bennett and Grimm.

$$a_{00} = (0.277 \pm 0.112)\left(\frac{\rho_G \langle v_G \rangle h_w}{\mu_L}\right)^{0.648 \pm 0.075} \times \left(\frac{A_{act}^2}{A_{open}^2} - 1\right)^{0.344 \pm 0.138} \left(\frac{\rho_L \mu_G}{\rho_G \mu_L}\right)^{0.412 \pm 0.079} \quad (23)$$

The intervals (uncertainties) of the parameters are reasonably small; furthermore, each parameter is positive with a probability exceeding 99.95%, conditional on the data and model used. The quality of this model is illustrated in Figure 7. The shape function $[(A_{act}/A_{open})^2 - 1]$ represents the relative kinetic energy increase of the gas as it approaches the holes.

The final two lines in Table 8 show the corresponding values of the objective function for the best individual fits of each data set, as calculated from the residual sums of squares in Tables 5, 6 and 7. The individual a_{00} functions fit the data significantly better than the overall models do; thus, some minor effects remain unexplained. Possible causes for these include: (i) differences in equipment or procedures of the three observer groups; (ii) physical mechanisms not yet included, such as Marangoni flows which were discussed in relation to Figure 5; and (iii) inaccuracies in the auxiliary correlations used. Having investigated several such possibilities (Young, 1990), we conclude that the present database does not justify going beyond Eq. 23.

Conclusion

The cross-flow tray model of Young and Stewart (1990) has been put into working form by providing Eq. 23 to predict the two-phase transfer function a_{00}. The correlations of Bennett and coworkers (1983, 1991) were used to predict the Peclet number *Pe* for liquid-phase dispersion on the tray. The parameters in Eq. 23 are closely determined, and the resulting tray model represents the selected data well, as shown in Figure 7. Extension of Eq. 23 is desirable, but will require a significantly broader database. We would like to hear about such data.

The correlations discussed in this work are based on binary data only. The FRI work included some multicomponent data, which were found to be well predicted by the method of Young and Stewart (1990) with Eq. 23 for a_{00}. Further testing of the method on multicomponent data is desirable.

Acknowledgment

This research was supported by Grant No. DE-FG02-84ER13291 from the U.S. Department of Energy, Office of Basic Energy Sciences, and by an AMOCO Foundation fellowship award to Thomas C. Young.

Notation

a_{00} = hydrodynamic function in Eqs. 11 and 13, dimensionless
A_0 = reference area for tray, m^2
A_{act} = active area of tray, m^2
A_{open} = open area of tray, m^2
A_{tray} = total projected area of tray, m^2
c = total concentration, kmol/m^3
$\mathfrak{D}_{AB}$ = binary diffusivity, m^2/s
d_h = hole diameter, m
e_0 = normal energy flux into given phase, relative to interface, W/m^2
h_w = outlet weir height, m
$k_A = k_B$ = binary molar transfer coefficient based on A_0, kmol/m^2/s
l^* = downstream coordinate for liquid relative to l_{tray}
l_{tray} = tray length in l direction, m
n_b = number of observations in data block b
N_{i0} = normal molar flux of species i into given phase, relative to interface and based on area A_0, kmol/m^2/s
N_{T0} = $(N_{A0} + N_{B0})$ for given binary phase, kmol/m^2/s
NPa = number of parameters used to represent a_{00}
$p(\theta|Y)$ = posterior probability density in θ space for given data Y, Eq. 19
$\mathfrak{R}$ = interfacial region on a tray
$s(u, w, t)$ = surface function in element of interfacial area, $s(u, w, t)\, du\, dw$, consistent units
$S'(\theta)$ = multiresponse objective function defined in Eq. 20
SS_b = sum of squares of residuals for data block b
t = time, s
u, w = imbedded interfacial coordinates
v = velocity, m/s
$\langle v_G \rangle$ = $w_G/(\rho_G A_{tray})$, characteristic velocity for vapor, m/s
$\langle v_L \rangle$ = $w_L/(\rho_L A_{tray})$, characteristic velocity for liquid, m/s
w = mass flow rate, kg/s
$\mathfrak{W}$ = molar flow rate, kmol/s
x = mole fraction in liquid
y = mole fraction in vapor
Y_b = column vector (data block) of observations from laboratory b
Y_{ub} = uth observation in vector Y_b
Y = array of all observations
z = vertical coordinate, m
θ = parameter vector in Eqs. 19–20
$\hat{\theta}$ = value of θ that maximizes $p(\theta|\mathbf{Y})$
μ = viscosity, kg/m/s
ν_b = degrees of freedom for data block b in Eq. 20
ρ = density, kg/m^3
$\phi_A = \phi_B$ = dimensionless net molar flux into given phase, N_{T0}/k_A

Dimensionless groups

Fr = $\langle v_G \rangle^2/(gh_w)$, Froude number
Pe = Peclet number for liquid

Re_G = $\rho_G\langle v_G\rangle h_w/\mu_G$, Reynolds number for vapor
Re_L = $\rho_L\langle v_L\rangle h_w/\mu_L$, Reynolds number for liquid
We = $\sigma/(\rho_L\langle v_G\rangle^2 d_h)$, Weber number

Subscripts

A,B = chemical species in a binary system
G = gas (vapor) phase
in, out = entering or leaving the tray
L = liquid phase
R = recycle stream
ref = reference value, normally taken at inlet
T = total over both species
0 = interfacial state
$0-, 0+$ = limits as $l^* \to 0$ from negative or positive values, respectively
∞ = bulk state

Superscripts

$*$ = dimensionless quantity
$\bullet$ = corrected for net molar interphase transfer

Functions and operations

$\text{erf}(\eta)$ = $(2/\sqrt{\pi}) \int_0^\eta \exp(-\eta_1^2)\, d\eta_1$, error function
$\langle f\rangle$ = average of f over A_{tray}

Literature Cited

Ahmed, I. S., "Computer-Aided Distillation Tray Design and Experimental Determination of Tray Efficiencies from a Semi-Industrial Distillation Column," PhD Diss., UMIST, Manchester, UK (1982).

American Institute of Chemical Engineers, *Bubble Tray Design Manual*, New York, (1958).

Anderson, R. H., G. R. Garrett, and M. Van Winkle, "Efficiency Comparison of Valve and Sieve Trays in Distillation Columns," *Ind. Eng. Chem. Proc. Des. Dev.*, **15**, 96 (1976).

Bakowski, S., "A New Method for Predicting the Plate Efficiency of Bubble-Cap Columns," *Chem. Eng. Sci.*, **1**, 266 (1952).

Bennett, D. L., R. Agrawal, and P. J. Cook, "New Pressure Drop Correlation for Sieve Tray Distillation Columns," *AIChE J.*, **29**, 434 (1983).

Bennett, D. L., and H. J. Grimm, "Eddy Diffusivity for Distillation Sieve Trays," *AIChE J.*, **37**, 589 (1991).

Box, G. E. P., and N. R. Draper, "The Bayesian Estimation of Common Parameters from Several Responses," *Biometrika*, **52**, 355 (1965).

Box, G. E. P., and G. C. Tiao, *Bayesian Inference in Statistical Analysis*, Addison-Wesley, Reading, MA (1973).

Box, M. J., and N. R. Draper, "Estimation and Design Criteria for Multiresponse Non-Linear Models with Nonhomogeneous Variance," *Appl. Statist.*, **21**, 13 (1972).

Brock, J. R., and R. B. Bird, "Surface Tension and the Principle of Corresponding States," *AIChE J.*, **1**, 174 (1955).

Caracotsios, M., "Model Parametric Sensitivity Analysis and Nonlinear Parameter Estimation," PhD Diss., Univ. of Wisconsin, Madison (1986).

Danckwerts, P. V., "Significance of Liquid-Film Coefficients in Gas Absorption," *Ind. Eng. Chem.*, **43**, 1460 (1951).

Draper, N., and H. Smith, *Applied Regression Analysis*, 2nd ed., Wiley, New York (1981).

Fane, A., and H. Sawistowski, "Surface Tension Effects in Sieve-Plate Distillation," *Chem. Eng. Sci.*, **23**, 943 (1968).

Földes, P., and I. Evangelidi, "Efficiency of Turbogrid-Tray Distillation Columns," *Brit. Chem. Eng.*, **13**, 1291 (1968).

Garrett, G. R., "Efficiency Prediction Method for Distillation Columns," PhD Diss., Univ. of Texas, Austin (1975).

Garrett, G. R., R. H. Anderson, and M. Van Winkle, "Calculation of Sieve and Valve Tray Efficiencies in Column Scale-Up," *Ind. Eng. Chem. Proc. Des. Dev.*, **16**, 79 (1977).

Gmehling, J., U. Onken, W. Arlt, P. Grenzheuser, U. Weidlich and B. Kolbe, "VLE Data Collection," Chemistry Data Ser. Vol. I, DECHEMA, Frankfurt (1977–1984).

Hausen, H., "A Definition of Exchange Efficiency of Rectifying Plates for Binary and Ternary Mixtures," *Chem. Ing. Tech.*, **25**, 595 (1953).

Higbie, R., "The Rate of Absorption of a Pure Gas into a Still Liquid during Short Periods of Exposure," *Trans. AIChE*, **31**, 365 (1935).

Hirschfelder, J. O., C. F. Curtiss, and R. B. Bird, *Molecular Theory of Gases and Liquids*, corrected printing with notes added, Wiley, New York (1964).

Hoek, P. J., and F. J. Zuiderweg, "Influence of Vapor Entrainment on Distillation Tray Efficiency at High Pressures," *AIChE J.*, **28**, 535 (1982).

Holland, C. D., *Multicomponent Distillation*, Prentice Hall, Englewood Cliffs, NJ (1963).

Holland, C. D., and K. S. McMahon, "Comparison of Vaporization Efficiencies with Murphree-Type Efficiencies in Distillation," *Chem. Eng. Sci.*, **25**, 431 (1970).

Hughmark, G. A., "Models for Vapor-Phase and Liquid-Phase Mass Transfer on Distillation Trays," *AIChE J.*, **17**, 1295 (1971).

Kalbassi, M. A., M. M. Dribika, M. W. Biddulph, S. Kler, and J. T. Lavin, "Sieve Tray Efficiencies in the Absence of Stagnant Zones," *Inst. Chem. Eng. Symp. Ser.*, **104**, A511 (1987).

King, C. J., *Separation Processes*, 2nd ed., McGraw Hill, New York (1980).

Krishna, R., "A Film Model Analysis of Nonequimolar Distillation of Multicomponent Mixtures," *Chem. Eng. Sci.*, **32**, 1197 (1977).

Krishna, R., "Model for Prediction of Point Efficiencies for Multicomponent Distillation," *Chem. Eng. R&D*, **63**, 312 (1985).

Krishnamurthy, R., and R. Taylor, "A Nonequilibrium Model of Multicomponent Separations Processes," *AIChE J.*, **31**, 449, 456, 1973 (1985).

Lockett, M. J., and I. S. Ahmed, "Tray and Point Efficiencies from a 0.6-m-Diametered Distillation Column," *Chem. Eng. Res. Des.*, **61**, 110 (1983).

Miskin, L. G., U. Ozlep, and S. R. M. Ellis, "Ternary Component Efficiency," *Brit. Chem. Eng. & Proc. Tech.*, **17**, 153 (1972).

Nord, M., "Plate Efficiencies of Benzene-Toluene-Xylene Systems in Distillation," *Trans. AIChE*, **42**, 863 (1946).

Oliver, E. D., and C. C. Watson, "Correlation of Bubble-Cap Fractionating-Column Plate Efficiencies," *AIChE J.*, **2**, 18 (1956).

Prausnitz, J. M., T. F. Anderson, E. A. Grens, C. A. Eckert, R. Hsieh, and J. P. O'Connell, *Computer Calculations for Multicomponent Vapor-Liquid and Liquid-Liquid Equilibria*, Prentice-Hall, Englewood Cliffs, NJ (1980).

Reid, R. C., J. M. Prausnitz, and B. E. Poling, *The Properties of Gases and Liquids*, 4th ed., McGraw-Hill, New York (1987).

Sakata, M., and T. Yanagi, "Performance of a Commercial Scale Sieve Tray," *Distillation: Inst. Chem. Eng. Symp. Ser.*, **56**, 3.2/21 (1979).

Standart, G., "Studies on Distillation—V," *Chem. Eng. Sci.*, **20**, 611 (1965).

Stewart, W. E., J. B. Angelo, and E. N. Lightfoot, "Forced Convection in Three-Dimensional Flows: II. Asymptotic Solutions for Mobile Interfaces," *AIChE J.*, **16**, 771 (1970).

Stewart, W. E., "Forced Convection: IV. Asymptotic Forms for Laminar and Turbulent Transfer Rates," *AIChE J.*, **33**, 2008 (1987).

Stewart, W. E., R. H. Shabaker, and Y. T. Lu, "Kinetics of Propylene Hydrogenation on Platinum-Alumina," *Chem. Eng. Sci.*, **43**, 2256 (1988).

Stewart, W. E., M. Caracotsios, and J. P. Sørensen, "GREG Software Package Documentation," Chem. Eng. Dept., Univ. of Wisconsin, Madison (1991).

Svehla, R. A., "Estimated Viscosities and Thermal Conductivities of Gases at High Temperature," NASA Tech. Rep. R-132, Lewis Research Center, Cleveland, OH (1962).

Tamura, M., M. Kurata, and H. Odani, "Viscosity of Pure Liquids," *Bull. Chem. Soc. Japan*, **28**, 83 (1955).

Tee, L. S., S. Gotoh, and W. E. Stewart, "Molecular Parameters for Normal Fluids," *Ind. Eng. Chem. Fund.*, **5**, 356 (1966).

Teja, A. S., and P. Rice, "Generalized Corresponding States Method for the Viscosities of Liquid Mixtures," *Ind. Eng. Chem. Fund.*, **20**, 77 (1981).

Toor, H. L., and J. K. Burchard, "Plate Efficiencies in Multicomponent Distillation," *AIChE J.*, **6**, 202 (1960).

Tyn, M. T., and W. F. Calus, "Diffusion Coefficients in Dilute Binary Liquid Mixtures," *J. Chem. Eng. Data*, **20**, 106 (1975).
Vignes, A., "Diffusion in Binary Solutions," *Ind. Eng. Chem. Fund.*, **5**, 189 (1966).
Wagner, W., "New Vapor Pressure Measurements for Argon and Nitrogen and a New Method for Establishing Rational Vapor Pressure Equations," *Cryogenics*, **13**, 470 (1973).
Wilke, C. R., "A Viscosity Equation for Gas Mixtures," *J. Chem. Phys.*, **18**, 517 (1950).
Yanagi, T., and M. Sakata, "Performance of a Commercial Scale 14% Hole Area Sieve Tray," *Ind. Eng. Chem. Proc. Des. Dev.*, **21**, 712 (1982).
Young, G. C., and J. H. Weber, "Murphree Point Efficiencies in Multicomponent Systems," *Ind. Eng. Chem. Proc. Des. Dev.*, **11**, 440 (1972).
Young, T. C., "Analysis and Applications of a Boundary-Layer Model for Multicomponent Crossflow Fractionation Trays," PhD Diss., Univ. of Wisconsin, Madison (1990).
Young, T. C., and W. E. Stewart, "Collocation Analysis of a Boundary-Layer Model for Crossflow Fractionation Trays," *AIChE J.*, **36**, 655 (1990).
Zuiderweg, F. J., and A. Harmens, "The Influence of Surface Phenomena on the Performance of Distillation Columns," *Chem. Eng. Sci.*, **9**, 89 (1958).

Appendix I: Physical Property Estimation Methods

Thermodynamic properties were calculated by the methods recommended by Prausnitz et al. (1980). The virial equation of state was used for the vapor phase and the UNIQUAC model for activities in the liquid phase. The mixture virial equation parameters, pure-fluid UNIQUAC parameters, and ideal-gas heat capacity polynomials were taken from Prausnitz et al. (1980). Vapor pressures were calculated from a version of the Wagner equation (1973) with parameters from Reid et al. (1987). UNIQUAC binary interaction parameters were estimated by the method described by Prausnitz et al. (1980), from vapor-liquid equilibrium data recommended by Gmehling et al. (1984).

Vapor-phase component viscosities and binary diffusivities were calculated from kinetic theory. Lennard-Jones potential parameters, based on viscosity data, were obtained from Tee et al. (1966), Hirschfelder et al. (1964), and Svehla (1962). Parameters for toluene were not available and were estimated using correlation (iii) of Tee et al. (1966). The collision integrals were adjusted for polar contributions as described by Reid et al. (1987). The Stefan-Maxwell multicomponent diffusion law was used for the vapor phase, and the mixing rule of Wilke (1950) was used to calculate vapor mixture viscosities. Soret and Dufour coefficients were neglected for both phases.

Liquid molar volumes were estimated from the modified Rackett equation and parameters given by Prausnitz et al. (1980). Pure liquid viscosities were normally calculated from four-parameter formulas given by Reid et al. (1987). We fitted three-parameter Andrade equations for *n*-heptane, *n*-butane and *i*-butane to viscosity data for these components. Liquid mixture viscosities were calculated by the corresponding-states method of Teja and Rice (1981).

Liquid binary diffusivities at infinite dilution were evaluated from experimental data, adjusted for temperature with the Stokes-Einstein equation. The method of Tyn and Calus (1975) was used when data at high dilution were not available. Binary diffusivities at higher concentrations were calculated by the method of Vignes (1966). Multicomponent diffusivities were calculated by the related method of Krishna (1977).

Pure-fluid surface tensions were evaluated from experimental data, with temperature corrections by the method recommended by Reid et al. (1987). The method of Brock and Bird (1955), as modified in Reid et al., was used when such data were not available. Mixture surface tensions for nonaqueous solutions were calculated from a thermodynamic relationship given by Reid et al., with activity coefficients of unity in the surface phase. Aqueous mixture surface tensions were calculated by the method of Tamura et al. (1955).

Appendix II: Comments and Corrections to the Previous Article

The following comments and corrections apply to the article of Young and Stewart (1991).

- In the Notation, read a as the interfacial area per unit volume of froth (vapor plus liquid).
- The superscripts I and II in Eqs. 1 through 6 should be removed. Their purpose is served by the subscripts G and L.
- In Eqs. 1 through 6, the interfacial fluxes are per unit interfacial area. From Eq. 7 on, the interfacial fluxes and transfer coefficients are per unit tray reference area A_0.
- The first and fifth equations under Eq. 10 should read as follows [asterisks (*) on the left for dimensionless velocities; stars (★) on the right for molar average velocities]:

$$v_G^* = v_G^{\star/V}$$

$$v_L^* = v_L^{\star/V}$$

- Numerical values of V_G and V_L are never needed, if Pe is given or is predicted from a version of Eq. 22. The working equations for the model use v_G^* and v_L^*, with specified inlet values (normally 1.0) for the latter functions.
- The correlations given here use the measurable characteristic velocities $\langle v_G \rangle$ and $\langle v_L \rangle$, in preference to the rather inaccessible quantities V_G and V_L. The Peclet number is defined here by Eqs. 3 and 7, equivalent to Pe of our 1990 article.

Manuscript received Dec. 27, 1990, and revision received Feb. 14, 1992.